Models of the Cytochromes *b*. Effect of Axial Ligand Plane Orientation on the EPR and Mössbauer Spectra of Low-Spin Ferrihemes

F. Ann Walker,*† Boi Hanh Huynh,*‡ W. Robert Scheidt,*§ and Sarah R. Osvath§

Contribution from the Department of Chemistry, San Francisco State University, San Francisco, California 94132, Department of Physics, Emory University, Atlanta, Georgia 30322, and Department of Chemistry, University of Notre Dame, Notre Dame, Indiana 46556.
Received October 24, 1985

Abstract: Combined Mössbauer, EPR, and structural studies of a series of well-defined low-spin heme model compounds have provided conclusive proof that so-called "strong g_{max}" EPR signals, in which g_{max} is greater than 3, can be correlated with near-axial symmetry and in the case of planar axial ligands with perpendicular alignment of ligand planes. These results have relevance to the understanding of a number of heme protein systems, including the membrane-bound *b* cytochromes of complex III of the respiratory chain of animals and of chloroplasts, which also have strong g_{max} EPR signals. The most extensive studies were conducted on the bis(2-methylimidazole) complex of iron(III) tetraphenylporphyrinate, $(TPP)Fe(2\text{-}MeImH)_2^+$. The low-temperature EPR and Mössbauer spectra of this complex in dimethylformamide solution are the same as those of the crystalline form for which the structure is known to have the axial ligands in perpendicular planes. Mössbauer spectral simulations of the spectrum of the DMF solution sample permit estimation of the other two (unobserved) *g* values [$g_y = 1.93$, $g_x = 0.85$; $g_y = 1.87$, $g_x = 0.82$], depending on assumptions. The large experimental value of g_z, 3.41, indicates that most of the molecules have their internal field oriented along the *z* axis of the **g** tensor. Hyperfine parameters determined for this sample include $A_z/g_n\beta_n = +810 \pm 50$ kG, $A_y/g_n\beta_n = +220 \pm 20$ kG, and $A_x/g_n\beta_n \sim -347$ kG (estimated from theoretical calculations). The structure of a new crystalline form of $(TPP)Fe(ImH)_2^+Cl^-$ has been determined. It contains two unique structural units, both of which have their imidazole ligands in parallel planes. In one molecular unit the dihedral angle between the imidazole planes and the porphyrin N_1-Fe-N_3 axis is 6°, and in the other it is 41°. The EPR spectrum of this crystalline form consists of two low-spin "B hemichrome" signals with slightly different *g* values, one set of which is the same as those observed for frozen solutions of the same complex. This suggests that one of the two orientations is thermodynamically favored. Crystal field and thermodynamic analyses, based upon reasonable estimates of the tetragonal and rhombic splittings of the d orbitals of low-spin Fe(III) porphyrins, suggest that perpendicular alignment of planar axial ligands could lead to a positive shift in redox potential of up to about 50 mV over that observed for parallel alignment, all other structural and environmental factors being equal. Thus, the frequent drop in redox potential and g_{max} value, observed when membrane-bound *b* cytochromes known to have two imidazole ligands are isolated from their complexes, are self-consistent and may suggest a change in protein conformation that allows the axial ligands to rotate from perpendicular to parallel alignment. However, the extremely positive redox potential observed for native chloroplast cytochrome b_{559} cannot be accounted for by axial ligand plane alignment alone.

There has long been considerable interest in determining what factors affect the redox potentials, electronic and magnetic resonance spectra of heme proteins, and in developing an understanding of how these physical properties may relate to each other and thus be useful in predicting the structural and electronic features of newly discovered heme proteins. Certainly, substituents on the β-pyrrole positions have long been known to affect the redox potentials and absorption maxima of the three major groups, the *a*-, *b*-, and *c*-type hemes,[1] all other things being equal. However, all other things usually are not equal, since these, as well as the EPR and NMR spectra and various other magnetic properties of the heme proteins, are further modulated by the nature of the axial ligands bound to the hemes. Cytochromes *c* are more often identified by their histidine/methionine axial ligand combination than by the covalent linkage between the 2- and 4-positions of the heme and two cysteine residues of the protein. However, more and more cases are emerging of bis(histidine) or 5-coordinate mono(histidine) coordination in cytochromes *c*, as in the cytochromes c_3[2-4] and *c*′,[4,5] respectively. Likewise, one often thinks of cytochromes *b* as being more closely identified with bis(imidazole) coordination than with the presence of the two vinyl groups of a noncovalently linked protoheme. However, cytochrome b_{562} from *Escherichia coli* has histidine/methionine coordination,[6] and hemoglobin, myoglobin, cytochrome P-450, catalase, peroxidase, and many others also contain the so-called *b*-type heme (extractable protoheme), yet have a variety of axial ligands.

Even within a common set of heme substituents and axial ligands, the physical properties of heme proteins vary widely. For example, among the cytochromes *b* that have bis(imidazole) coordination are found cytochromes b_5 from liver[7,8] and erythrocytes[9,10] of animals and yeast flavocytochrome b_2,[11,12] all of whose heme centers have redox potentials in the range 0 to +30 mV vs. NHE. They also have well-characterized and very similar NMR spectra and EPR spectra characteristic of "class B" heme proteins, with $g_1 = 2.9$, $g_2 = 2.2$, and $g_3 = 1.5$.[13-15] Also within this class

† San Francisco State University.
‡ Emory University.
§ University of Notre Dame.

(1) Falk, J. E. *Porphyrins and Metalloporphyrins*; Elsevier: New York, 1964; p 70.
(2) Pierrot, M.; Haser, R.; Frey, M.; Payan, F.; Astier, J.-P. *J. Biol. Chem.* **1982**, *257*, 14341-14348.
(3) Higuchi, Y.; Bando, S.; Kusuniki, M.; Matsuura, Y.; Yasuoka, N.; Kakudo, M.; Yamanaka, T.; Yagi, T.; Inokuchi, H. *J. Biochem. (Tokyo)* **1981**, *89*, 1659-1662.
(4) Mathews, F. S. *Prog. Biophys. Mol. Biol.* **1985**, *45*, 1-56.
(5) Weber, P. C.; Howard, A.; Xuong, N. H.; Salemme, F. R. *J. Mol. Biol.* **1981**, *153*, 399-424.
(6) Mathews, F. S.; Bethge, P.; Czerwinski, E. W. *J. Biol. Chem.* **1979**, *254*, 1699-1706.
(7) Mathews, F. S.; Czerwinski, E. W.; Argos, P. In *The Porphyrins*; Dolphin, D., Ed.; Academic: New York, 1979; Vol. 7, pp 108-147.
(8) Weber, H.; Weiss, W.; Staudinger, H. *Hoppe-Seyler's Z. Physiol. Chem.* **1971**, *352*, 109-110.
(9) Passon, P. G.; Reed, D. W.; Hultquist, D. E. *Biochim. Biophys. Acta* **1972**, *275*, 51-61.
(10) Iyanagi, T. *Biochemistry* **1977**, *16*, 2725-2730.
(11) Keller, R.; Groudinsky, O.; Wuthrich, K. *Biochim. Biophys. Acta* **1973**, *328*, 233-238.
(12) Labeyrie, F.; Groudinsky, O.; Jacquot-Armand, Y.; Naslin, L. *Biochim. Biophys. Acta* **1966**, *128*, 492-503.
(13) Watari, H.; Groudinsky, O.; Labeyrie, F. *Biochim. Biophys. Acta* **1967**, *131*, 589-592.
(14) Bois-Poltoratsky, R.; Ehrenberg, A. *Eur. J. Biochem.* **1967**, *2*, 361-365.
(15) Blumberg, W. E.; Peisach, J. In *Structure and Bonding of Macromolecules and Membranes*; Chance, B., Yonetani, T., Eds.; Academic: New York, 1971; p 215.

0002-7863/86/1508-5288$01.50/0

Table I. Axial Ligand Bond Lengths, Ligand Plane Orientations, and Spin States in Fe(III) Porphyrin Complexes, $[Fe(por)L_2]^+$

por	L	φ,[a] deg	Θ,[b] deg	Fe–N_{ax}, Å	spin state	ref
proto IX	*N*-MeIm	−3, 16	19	1.975 (av)	LS	32
OEP	2-MeImH	22	0[c]	2.275	HS	33
OEP	3-Clpy	41	0[c]	2.043 LS 2.316 HS	HS–LS equil	34a
OEP	3-Clpy	av 9.5 ± 2 (4 values)	2 (2 values)	2.310 (av)	IS	34b
OEP	3-Clpy	7.4 ± 2 (2 values)	2.6	2.304 (av)	IS	34c
TPP	BzimH	10	0[c]	2.216	HS	35
TPP	4-MeIm	1, 17	18	1.928, 1.958	LS	36
TPP	ImH	−18, 39	57	1.957, 1.991	LS	37
TPP	2-MeImH	−58, 32	89	2.013 (av)	LS	38

[a] The φ angle is the dihedral angle between the imidazole or pyridine plane and the coordinate plane containing N_1 and N_3. [b] Dihedral angle between the two imidazole or pyridine planes. [c] Value of 0° required by crystallographic symmetry.

are a wide variety of membrane-bound cytochromes *b*, including mitochondrial b_{566} (b_T) and b_{562} (b_K), chloroplast b_6, and chloroplast b_{559}, which have also been shown to have bis(imidazole) coordination to the heme.[16,17] However, these proteins have a wider range of redox potentials than the b_5 and b_2 group,[18-26] and they are all further characterized by a peculiar EPR signal, having a strong g_{max} feature at $g > 3.3$ as the sole observable spectral feature.[20-27] We[28,29] and others[16,24,30,31] have speculated that this signal is due to the axial imidazole planes being maintained perpendicular to each other rather than parallel as in cytochrome b_5.[7] This raises the question of whether large values of g_{max} may be correlated with high redox potentials, a question that we will address in the Discussion. It also raises the question as to how one might prove, utilizing a series of well-defined model compounds, whether a definite relationship exists between axial ligand plane orientation and spectroscopic (and redox) properties.

Numerous structures of model Fe(III) porphyrins coordinated to imidazoles have long indicated the propensity of the axial ligands to adopt a seemingly unfavorable orientation lying over or very close to the N_1–N_3 porphyrin vector and when two imidazole (or pyridine) ligands are present, to maintain their axial ligands in nearly parallel planes.[26,32-38] In Table I are summarized the structural and bulk magnetic data for those bis(imidazole) or bis(pyridine) complexes of model hemins.[32-38] It is interesting to note that, in the majority of cases reported,[32-37] the two axial ligands not only are close to eclipsing the N_1–N_3 axis but also in all but two cases[37,38] are coplanar or nearly so. In only one case published so far, that of $(TPP)Fe(2\text{-}MeImH)_2^+$,[38] are the axial ligands in perpendicular planes. In comparing the structures of $(TPP)Fe(ImH)_2^+$[37] and $(TPP)Fe(2\text{-}MeImH)_2^+$,[38] the striking feature is the close similarity in the Fe–N_{ax} bond lengths, despite the expected steric hindrance of the 2-methyl groups of the latter complex. This steric hindrance is alleviated in part by the rotation of the 2-methylimidazole planes so that their projection on the porphyrin ring creates angles of 32° with the N_1–N_3 and N_2–N_4 vectors, respectively.[38,39] Both bis(imidazole) complexes of $(TPP)Fe^{III}$ have been shown to be low spin in the solid state and/or in solution: Scheidt and co-workers[40,41] have reported the magnetic susceptibility of crystalline $(TPP)Fe(2\text{-}MeImH)_2^+ClO_4^-$ and of this and several other complexes in solution;[40,41] LaMar and coworkers[42] have also reported the solution magnetic susceptibilities of all of these complexes, measured by the Evans method at −20 °C. Furthermore, the NMR spectra of all three complexes at room temperature have the pyrrole H signal upfield from Me_4Si.[42-45] consistent with a low-spin d^5-electron configuration.

Despite the similarity in magnetic susceptibility and NMR results, low-temperature EPR spectra of glassy samples of $(TPP)Fe(ImH)_2^+I^-$, $(TPP)Fe(N\text{-}MeIm)_2^+I^-$, and $(TPP)Fe(2\text{-}MeImH)_2^+I^-$ in $CHCl_3$, CH_2Cl_2, and DMF have indicated marked differences between the hindered and nonhindered bis(imidazole) complexes:[29] observable up to ca. 100 K, with characteristic *g* values of 2.87, 2.29, and 1.56, while $(TPP)Fe(2\text{-}MeImH)_2^+I^-$ has a strong g_{max}, previously called "HALS" (highly anisotropic low spin),[46] EPR signal, observable only below 30 K and consisting of one strong feature at $g = 3.4$ and a broad tail extending to at least 10 000 G at X-band. Taking the minimum in the broad tail as the highest field *g* value and assuming $\sum g^2 = 16.0$, the following parameters were reported for $(TPP)Fe(2\text{-}MeImH)_2^+I^-$: $g_1 = 3.4$, $g_2 = 1.74$, $g_3 = 1.19$.[29] Similar spectra were observed for the bis(ligand) complexes of $(TPP)Fe^{III}$ with 1,2-dimethylimidazole, 5,6-dimethylbenzimidazole, and low-basicity pyridines.[29] Since these were glassy EPR samples, the orientation of the axial ligand planes in these complexes was unknown, and untested extrapo-

(16) Widger, W. R.; Cramer, W. A.; Herrmann, R. G.; Trebst, A. *Proc. Natl. Acad. Sci. U.S.A.* **1984**, *81*, 674–678.
(17) Babcock, G. T.; Widger, W. R.; Cramer, W. A.; Oertling, W. A.; Metz, J. *Biochemistry* **1985**, *24*, 3638–3645.
(18) Erecinska, M.; Oshino, R.; Oshino, N.; Chance, B. *Arch. Biochem. Biophys.* **1973**, *157*, 431–445.
(19) Nelson, B. D.; Gellerfors, P. *Biochim. Biophys. Acta* **1974**, *357*, 358–364.
(20) Leigh, J. S.; Erecinska, M. *Biochim. Biophys. Acta* **1975**, *387*, 95–106.
(21) Von Jagow, G.; Schagger, H.; Engel, W. D.; Hachenberg, H.; Kolb, H. J. C. In *Energy Conservation in Biological Membranes*; Schafer, G., Klingenberg, M., Eds.; Springer: Berlin, 1978; pp 43–52.
(22) Salerno, J. C. *J. Biol. Chem.* **1984**, *259*, 2331–2336.
(23) T'sai, A.-H.; Palmer, G. *Biochim. Biophys. Acta* **1983**, *722*, 349–363.
(24) T'sai, A.; Palmer, G. *Biochim. Biophys. Acta* **1982**, *681*, 484–495.
(25) Salerno, J. C. *FEBS Lett.* **1983**, *162*, 257–261.
(26) Malkin, R.; Vanngard, T. *FEBS Lett.* **1980**, *111*, 228–231.
(27) Orme-Johnson, N. R.; Hansen, R. E.; Beinert, H. *J. Biol. Chem.* **1974**, *249*, 1928–1939.
(28) Scheidt, W. R.; Chipman, D. M. *J. Am. Chem. Soc.* **1986**, *108*, 1163–1169.
(29) Walker, F. A.; Reis, D.; Balke, V. L. *J. Am. Chem. Soc.* **1984**, *106*, 6888–6898.
(30) Carter, K. R.; T'sai, A.; Palmer, G. *FEBS Lett.* **1981**, *132*, 243–246.
(31) Palmer, G. *Biochem. Soc. Trans.* **1985**, *13*, 548–560.
(32) Little, R. G.; Dymock, K. R.; Ibers, J. A. *J. Am. Chem. Soc.* **1975**, *97*, 4532–4539.
(33) Geiger, D. K.; Lee, Y. J.; Scheidt, W. R. *J. Am. Chem. Soc.* **1984**, *106*, 6336–6343.
(34) (a) Scheidt, W. R.; Geiger, D. K.; Haller, K. J. *J. Am. Chem. Soc.* **1982**, *104*, 495–499. (b) Scheidt, W. R.; Geiger, D. K.f Hayes, R. G.; Lang, G. *J. Am. Chem. Soc.* **1983**, *105*, 2625–2632. (c) Scheidt, W. R., unpublished work.
(35) Levan, K. R.; Strouse, C. E. *Abstracts of Papers*, American Crystallographic Association Summer Meeting, Snowmass, CO, American Crystallographic Association: New York, 1983; Abstract III. Levan, K. R. Ph.D. Thesis, University of California at Los Angeles, 1984.
(36) Quinn, R.; Strouse, C. E.; Valentine, J. S. *Inorg. Chem.* **1983**, *22*, 3934–3940.
(37) Collins, D. M.; Countryman, R.; Hoard, J. L. *J. Am. Chem. Soc.* **1972**, *94*, 2066–2072.
(38) Kirner, J. F.; Hoard, J. L.; Reed, C. A. *Abstracts of Papers*, 175th National Meeting of the American Chemical Society, Anaheim, CA, March 13–16, 1978; American Chemical Society: Washington, DC, 1978; INOR 14.
(39) Hoard, J. L., personal communication.
(40) Scheidt, W. R.; Geiger, D. K., unpublished data. Solution susceptibilities are given in ref 33.
(41) The importance of comparing all physical properties on complexes in the solid state is shown by the differences in magnetic moments of $(OEP)Fe(2\text{-}MeImH)_2^+ClO_4^-$ in the solid state and in solution.
(42) Satterlee, J. D.; LaMar, G. N.; Frye, J. S. *J. Am. Chem. Soc.* **1976**, *98*, 7275–7282.
(43) LaMar, G. N.; Walker, F. A. *J. Am. Chem. Soc.* **1973**, *95*, 1782–1790.
(44) LaMar, G. N.; Walker, F. A. In *The Porphyrins*; Dolphin, D., Ed.; Academic: New York, 1979; Vol. 4, pp 61–157.
(45) Walker, F. A. *J. Am. Chem. Soc.* **1980**, *102*, 3254–3256.
(46) Migita, C. T.; Iawizumi, M. *J. Am. Chem. Soc.* **1981**, *103*, 4378–4381.

lations from the crystal state to glassy solution are not warranted, as will become abundantly clear below.

Preliminary Mössbauer spectral measurements[47] also indicated a subtle difference in the magnetic behavior of the low-spin bis(ligand) complexes of hindered and nonhindered imidazoles with (TPP)Fe^{III}: At 4.2 K (TPP)Fe$(ImH)_2^+Cl^-$ and (TPP)Fe-$(N\text{-}MeIm)_2^+Cl^-$ had broad, unresolved hyperfine envelopes, while the spectrum of (TPP)Fe$(2\text{-}MeImH)_2^+Cl^-$ consisted of six reasonably well-resolved hyperfine lines in the absence of a magnetic field. Part of the impetus of the present work was to investigate in detail this Mössbauer signal in order to determine whether it could provide interpretive information concerning the strong g_{max} signal, which might, in turn, be related to structural differences between bis(ligand) complexes of hindered and nonhindered imidazoles. The results suggested the importance of measuring the EPR and Mössbauer spectra of the crystalline form of (TPP)-Fe$(2\text{-}MeImH)_2^+ClO_4^-$, whose structure has been reported by Hoard,[38] which we have done as part of this work. As will become clear, this compound holds an important key for interpreting the nature of the heme environment in the cytochromes *b* of complex III and other heme proteins having bis(histidine) coordination that exhibit a strong g_{max} signal. The results also point out the key role of Mössbauer spectroscopy in obtaining the *g* values needed for this interpretation.

Experimental Section

Iron-57 metal (95.45% enriched) was purchased from New England Nuclear and was oxidized to Fe(II) by stirring and heating (80 °C) 100 mg for 3 h under nitrogen in 100 mL of glacial acetic acid into which dry HCl gas was bubbled for the first 10 min. Upon complete solution of the iron metal, the glacial acetic acid solution containing the $^{57}Fe(II)$ was added to a degassed solution containing 100 mL of glacial acetic acid and 100 mL of pyridine that contained 2.5 g of tetraphenylporphyrin-free base ($TPPH_2$). After the solution was heated and stirred for another 1 h under nitrogen, the nitrogen was turned off and heating and stirring were continued for 12 h. The porphyrinic material was isolated by adding ca. 200 mL of methylene chloride and pouring the resulting solution through ca. 700 mL of distilled water three times in a separatory funnel without shaking; it was then washed with distilled water three times in the separatory funnel with shaking, dried over Na_2SO_4, evaporated to dryness, and chromatographed on silica gel (Baker chromatographic grade). The unreacted $TPPH_2$ was eluted with methylene chloride, and the iron-containing fractions were eluted with 5% methanol/methylene chloride. The iron-containing fractions were combined and evaporated to dryness; the resultant material was dissolved in benzene, dry HCl gas was bubbled through, and the solution was evaporated to dryness. The sample was rechromatographed on silica gel and eluted with 5% methanol/methylene chloride several additional times, evaporated to dryness, redissolved in benzene, bubbled with dry HCl, and reevaporated to dryness before Mössbauer samples were prepared.

Solution samples for Mössbauer and EPR spectroscopies were prepared by weighing out ca. 82 mg of 2-methylimidazole (2-MeImH) and diluting it to 5 mL with spectroscopic grade dimethylformamide (DMF) (Matheson, Coleman, Bell). This solution was added to ca. 10 mg of (TPP)$^{57}FeCl$ just before placement in the Mössbauer and EPR sample holders, and the resulting samples were frozen immediately in liquid nitrogen. The Mössbauer solution sample had a volume of 0.4 mL, with a concentration of approximately 2.5 mM (TPP)Fe$(2\text{-}MeIm)_2^+$ in DMF. Crystalline samples for Mössbauer and EPR spectroscopies were not enriched in ^{57}Fe. The Mössbauer spectrometer is of the constant-acceleration type. The zero velocity is referred to the centroid of room-temperature Mössbauer spectra of a metallic iron foil. The EPR measurements were performed with a Varian E-109 spectrometer at the laboratory of Dr. D. V. DerVartanian at the University of Georgia or with an IBM Instruments spectrometer at Emory University. Both the EPR and the Mössbauer spectrometers have been described elsewhere.[48] Some of the EPR measurements were carried out at San Francisco State University with a Varian E-12 spectrometer equipped with an Air Products flowing liquid-helium Dewar system from R. G. Hansen & Associates. The S-band EPR spectrum was recorded at the EPR Center at the Medical College of Wisconsin.

Crystals of low-spin iron(III) porphyrins were prepared by reaction of various Fe(Por)Y complexes with a 3- to 5-fold excess of nitrogenous base in THF, halocarbon, or aromatic solvent. The resulting solutions were allowed to slowly evaporate until crystallization occurred. In several cases, the iron(III) porphyrinate starting material rather than the desired adduct was obtained. For those complexes having sterically hindered imidazole ligands, a large fraction of these showed high-spin EPR spectra and are not further discussed in this paper.

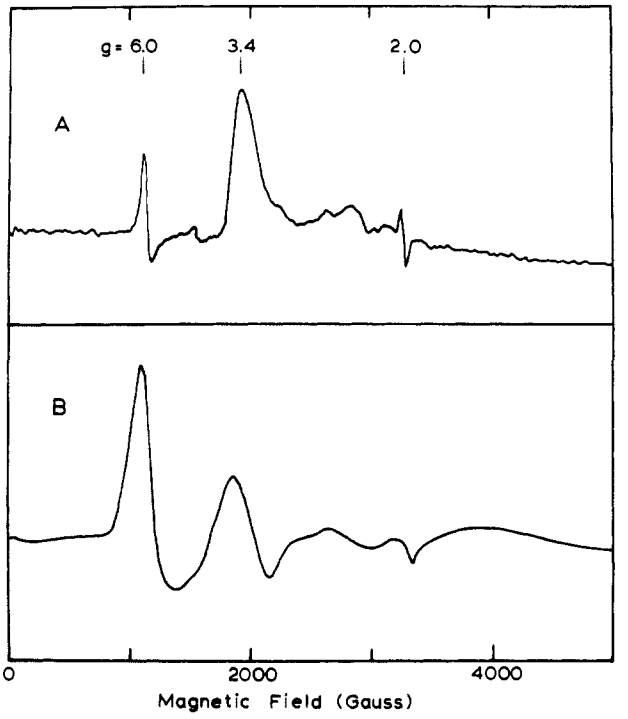

Figure 1. EPR spectra of (TPP)Fe$(2\text{-}MeImH)_2^+$: (A) DMF glass; (B) crystalline form. The Fe(III) concentration in DMF was 5 mM, and the sample was 94% enriched in ^{57}Fe. The crystals were not enriched in ^{57}Fe. They were suspended in mineral oil. Experimental conditions: (A) 0.2-mW power at 13 K and 9.162-GHz microwave frequency with 10-G modulation and 3.2×10^4 gain; (B) 10 mW at 6 K and 9.249 GHz with 10-G modulation and 3.2×10^2 gain. The high-spin Fe(III) impurity signal at $g = 6$ is due to ca. 15% of the iron present (see Figure 4 and text) but appears as an intense signal due to the much greater transition probability for this species than for the strong g_{max} species whose signal appears at $g = 3.4$.

Results

EPR. Figure 1A shows an EPR spectrum of (TPP)Fe$(2\text{-}MeImH)_2^+$ in DMF recorded at 13 K. The spectrum exhibits a dominant signal at $g_z = 3.41$, typical of the strong g_{max} type ferric heme compound.[29,46] The line width of this signal is about 240 G, at X-band, and narrows to about 56 G at S-band (2.355 GHZ), indicating that the iron environment is inhomogeneous. Signals corresponding to g_x and g_y are not observed at either X-band or S-band. It appears that these signals are broadened beyond recognition. The following Mössbauer study suggests that $g_x = 0.82\text{–}0.85$ and $g_y = 1.87\text{–}1.93$. Values of $g_y = 2.2\text{–}2.3$ for a series of strong g_{max} type ferric heme compounds have been reported previously by Migita and Iwaizumi;[46] however, the intensities of those reported g_y signals were substantially smaller than that of the g_z signals. It was demonstrated by Carter et al.[30] that the reported g_y signals represent minor low-spin ferric impurities in the samples. From Figure 1A it is obvious that our sample contains insignificant amounts of low-spin species with $g = 2.2$. The spectrum shown in Figure 1A also exhibits signals at $g = 6.0$ and 2.0, indicating that the sample contains small amounts of high-spin ferric heme and free-radical impurities.

For comparison, the EPR spectra of two different crystalline forms of (TPP)Fe$(2\text{-}MeImH)_2^+$ were measured. Both have essentially identical spectra, and the spectrum of one crystalline form is shown in Figure 1B. The crystals of (TPP)Fe$(2\text{-}MeImH)_2^+$ obtained from THF solution have the same space group and unit cell constants as those crystals from which the structure (Table I) was derived. A second crystalline phase was obtained as a

(47) Walker, F. A.; Parak, F., unpublished work data.
(48) Huynh, B. H.; Lui, M. C.; Moura, J. J. G.; Moura, I.; Ljungdahl, P. O.; Munck, E.; Payne, W. J.; Peck, H. D., Jr.; DerVartanian, D. V.; LeGall, J. *J. Biol. Chem.* **1982**, *257*, 9576–9581.

Table II. Pertinent Bond Lengths and Axial Ligand Plane Orientation Angles for Newly Determined (TPP)FeL_2^+ Structures and Their Comparison to Those of (TPP)Fe(2-MeImH)$_2^+$

por	L	φ,[a] deg	θ,[b] deg	Fe–N_{ax}, Å	spin state	ref
TPP	ImH	6	0[c]	1.977	LS	49, this work
		41	0[c]	1.964	LS	49, this work
TPP	2-MeImH	−58, 32	89	2.015	LS (strong g_{max})	38

[a] The φ angle is the dihedral angle between the imidazole plane and the coordinate plane containing N_1 and N_3. [b] Dihedral angle between the two imidazole planes. [c] Value of 0° required by crystallographic symmetry.

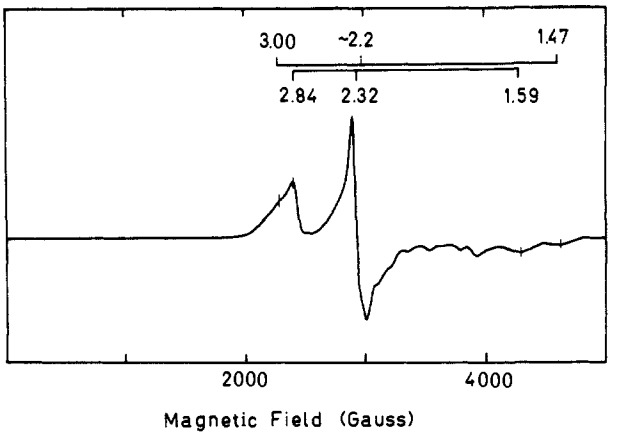

Figure 2. EPR spectrum of a small number of crystallites of (TPP)Fe(ImH)$_2^+$Cl$^-$ of the same batch from which the structure described in Table II was determined. Recording conditions were the same as those of Figure 1B. Because of the small number of crystallites, a true powder EPR spectral shape was not achieved, as evidenced by the additional bumps between 3200 and 4100 G. The relevant g values of the two species are grouped above the spectrum, on the basis of the Griffith condition that $\sum g^2 \sim 16$.[51]

chloroform solvate; it has the same space group and nearly identical cell constants and is presumed to be isostructural with the first (THF) solvate. A strong, broad signal, which peaks at $g = 3.56$, is observed for both crystalline samples. Signals originating from multiple minor species are also observed. The intense signal at $g = 6.0$ indicates that the crystal contains a substantial amount (ca. 15%, estimated from the Mössbauer spectrum) of high-spin ferric heme impurities. Nevertheless, similar to the sample in DMF solution, the major species in the crystalline sample is the strong g_{max} type ferric heme compound[46] that exhibits a single strong signal in the $g = 3.3$–3.6 region.

The EPR spectra of a series of other crystalline samples of low-spin (TPP)FeL_2^+ complexes were surveyed to determine how EPR spectral parameters related to molecular structure. Two interesting cases were found, the results of which are included in this report: Crystals of (TPP)Fe(ImH)$_2^+$Cl$^-$ with a space group different from that reported by Hoard and co-workers[37] showed what appeared to be two overlapping "normal" EPR spectra, with $g_z = 3.00$, $g_y \approx 2.2$, $g_x = 1.47$ and $g_z = 2.84$, $g_y = 2.32$, $g_x = 1.59$ (Figure 2); crystals of [(p-OCH$_3$)$_4$TPP]Fe(benzImH)$_2^+$ClO$_4^-$ showed a single signal at $g = 3.51$. The first structure has been solved, and the detailed description of the structure will be published elsewhere.[49] The features pertinent to interpretation of the EPR and Mössbauer data are summarized in Table II, where the bond lengths and axial ligand plane orientations are compared to those of (TPP)Fe(2-MeImH)$_2^+$. Crystals of the second complex are not of adquate quality for structure determination. Further work is continuing.

An additional EPR experiment involved crystals of (OEP)Fe(2-MeIm)$_2^+$ClO$_4^-$, which is high spin in the solid state and has parallel orientation of axial ligand planes.[33] In the solid state, even at 11 K, the only EPR signal observed is that of a high-spin ferric heme, with a slight rhombic splitting ($g_1 = 7.11$, $g_2 = 6.45$, $g_3 \sim 1.97$), as shown in Figure 3A. However, when these crystals are dissolved in CH_2Cl_2 and the glassy spectrum is recorded at low temperatures (11 K), both this high-spin signal and a strong g_{max} signal were observed (Figure 3B), the latter with $g_{max} = 3.56$ and no clear evidence of other components. Addition of 2-methylimidazole to (OEP)FeClO$_4$ in CHCl$_3$ and cooling to 7 K produced EPR signals due to a small amount of high-spin Fe(III) porphyrin ($g_\perp = 6.21$), but the majority of the sample had a strong g_{max} signal, with $g = 3.54$ (Figure 3C). Similar glassy samples, with the axial ligands being pyridine and 5,6-dimethylbenzimidazole, gave similar low-temperature spectra with $g_{max} = 3.43$ and 3.51, respectively, slightly larger g_{max} values in all three cases than the corresponding TPP complexes reported earlier.[29]

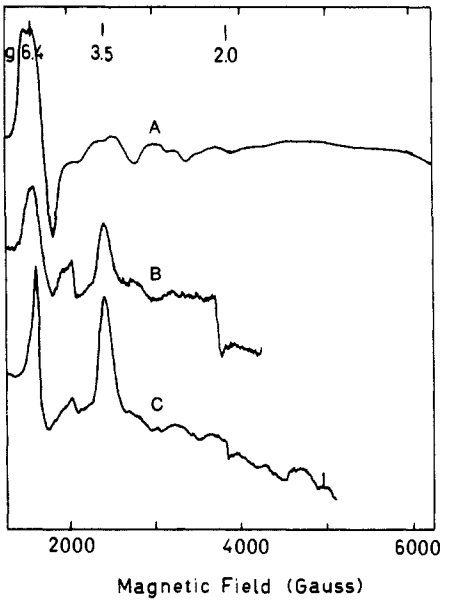

Figure 3. EPR spectra of (OEP)Fe(2-MeImH)$_2^+$ClO$_4^-$: (A) crystalline form; (B) crystals dissolved in methylene chloride; (C) the same solution with additional 2-MeIm added. Spectra were recorded at 11 K under conditions similar to those of Figure 1. In (A), the additional features between $g = 6$ and $g = 2$ are due to the fact that only a few crystals were used for this spectrum, and hence a true random distribution of orientations of crystallites was not achieved.

Mössbauer Spectra. Figure 4 shows Mössbauer spectra of (TPP)Fe(2-MeImH)$_2^+$ in DMF (Figure 4A) and in the crystalline form (Figure 4B). The data were recorded at 150 K. Both spectra exhibit an intense quadrupole doublet. Least-squares fits of the data yield parameters for the quadrupole splitting $\Delta E_Q = 1.71 \pm 0.02$ mm/s and isomer shift $\delta = 0.21 \pm 0.02$ mm/s for the frozen solution sample and $\Delta E_Q = 1.77 \pm 0.03$ mm/s and $\delta = 0.22 \pm 0.03$ mm/s for the crystalline sample. These parameters are typical for low-spin ferric samples. These samples have also been studied at 100 K. It was found that within experimental uncertainties the quadrupole splittings are temperature independent. The spectrum in Figure 4B also shows that the crystalline sample contains approximately 15% high-spin ferric impurity, indicated by a small peak at +0.05 mm/s and a shoulder at +0.86 mm/s. A similar type of high-spin ferric impurity is also observed in spectrum 4A. The percentage of this impurity in the solution sample is estimated to be less than 5%.

Figure 5 shows Mössbauer spectra of (TPP)Fe(2-MeImH)$_2^+$ in DMF recorded at 4.2 K with an external magnetic field of 500 G applied perpendicular (Figure 5A) and parallel (Figure 5B)

(49) Scheidt, W. R.; Osvath, S. R.; Lee, Y. J., to be submitted for publication. The complex has the formula (TPP)Fe(ImH)$_2^+$Cl$^-$·H$_2$O·CHCl$_3$. The space group is $P\bar{1}$ with cell constants $a = 13.331$ (2) Å, $b = 17.688$ (3) Å, $c = 11.212$ (2) Å, $\alpha = 107.99$ (1)°, $\beta = 94.701$ (1)°, $\gamma = 69.68$ (1)°, and $Z = 2$.

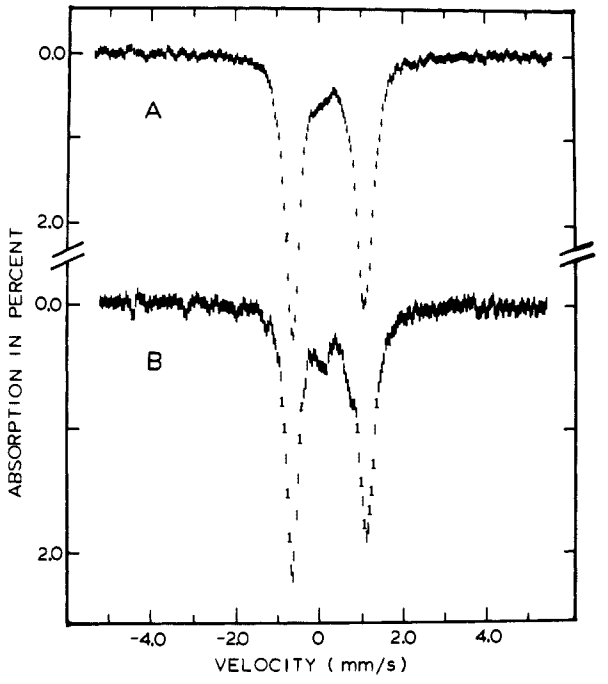

Figure 4. Mössbauer spectra of $(TPP)Fe(2\text{-}MeImH)_2^+$ in DMF (A) and in crystalline form (B) recorded at 150 K without external magnetic field. In spectrum B the small peak at +0.05 mm/s and a shoulder at +0.86 mm/s indicate that the crystalline sample contains appreciable amounts (ca. 15%) of high-spin ferric impurity.

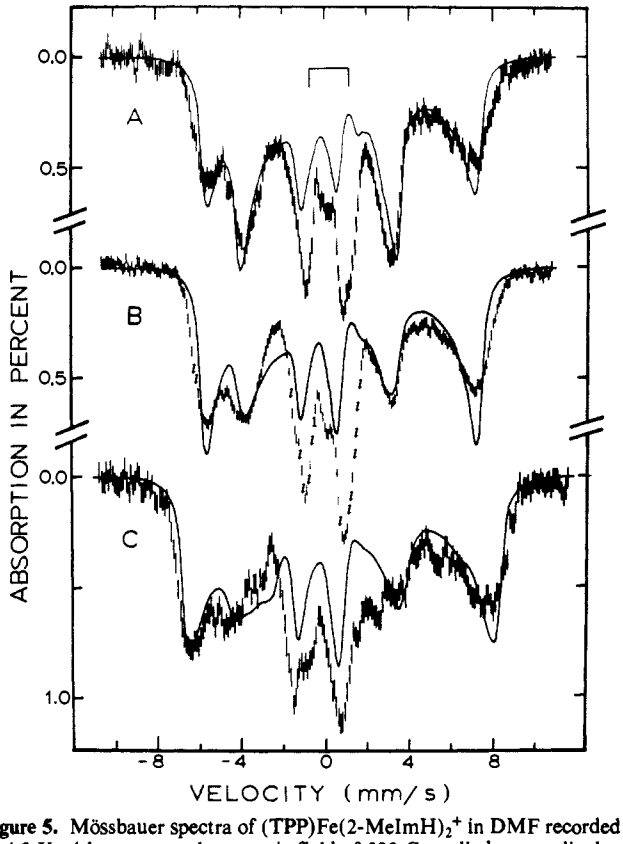

Figure 5. Mössbauer spectra of $(TPP)Fe(2\text{-}MeImH)_2^+$ in DMF recorded at 4.2 K with an external magnetic field of 500 G applied perpendicular (A) and parallel (B) to the γ-beam and with a parallel field of 60 kG (C). The solid lines are theoretical spectra generated with the parameter set listed in column 3 of Table III. The bracket in (A) indicates positions of a quadrupole doublet resulting from a fast-relaxing, low-spin ferric species.

to the γ-beam, and with a parallel field of 60 kG (Figure 5C). Magnetic spectra with well-resolved hyperfine lines are observed at this temperature, in distinction to those of more typical low-spin

Table III. Crystal Field and Hyperfine Parameters of $(TPP)Fe(2\text{-}MeImH)_2^+$ in Dimethylformamide

		theory	
	experiment	$k = 1$	$\sum g^2 = 16$
$\Delta/k\lambda$[a]		2.96	2.88
$V/k\lambda$		0.88	0.92
k		1.00	1.02
g_x		0.82	0.85
g_y		1.87	1.93
g_z	3.41 (5)[b]	3.41	3.41
$A_x/g_n\beta_n$,[c] kG	−347[d]	−344	−350
$A_y/g_n\beta_n$,[c] kG	+220 (50)[b]	+218	+225
$A_z/g_n\beta_n$,[c] kG	+810 (20)[b]	+814	+795
ΔE_Q,[e] mm/s	+1.71 (2)[b]	+2.83	+2.87
δ,[e] mm/s	+0.21 (2)		
η[f]	−2.0 (5)[b]	−1.96	−2.02

[a] The proper axis system was adopted such that $|V/\Delta| \leq {}^2/_3$. [b] Numbers in parentheses given the uncertainties in units of the least significant digit. The uncertainties in the hyperfine parameters were estimated by visually comparing the data with theoretical Mössbauer spectra computer from eq 1. [c] The gyromagnetic ratio, g_n, has the values 0.1806 and −0.1033 for the ground and excited states of the ^{57}Fe nucleus. [d] The Mössbauer spectra are insensitive to this parameter. The theoretical value is therefore used to simulate the spectra. [e] 150 K value. [f] $\eta = (V_{xx} - V_{yy})/V_{zz}$, where V_{ii} are the components of the electric field gradient tensor.

Fe(III) porphyrins such as $(TPP)Fe(Im)_2^+$.[47] These well-resolved hyperfine spectra can be analyzed by a spin Hamiltonian as in eq 1, where S is the fictitious spin $^1/_2$ associated with the ground Kramers's doublet. All symbols in eq 1 have their conventional meaning.

$$\hat{H} = \beta_e\vec{S}\cdot\tilde{g}\cdot\vec{H} + \vec{S}\cdot\vec{A}\cdot\vec{I} + (eQV_{zz}/12)[3I_z^2 - I(I+1) + \eta(I_x^2 - I_y^2)] + g_n\beta_n\vec{H}\cdot\vec{I} \quad (1)$$

Since the measured g_z value, 3.41, is large, most of the molecules have their internal field oriented along the principal z axis of the **g** tensor. The observed spectra are basically determined by the z components of the **g** tensor, g_z, the magnetic hyperfine **A** tensor, A_z, and the electric field gradient tensor, V_{zz}. Consequently, these components can be determined experimentally with high accuracy. In order to gain information for the other parameters, we use eq 1 to simulate Mössbauer spectra and compare them with the experimental spectra. The solid lines in Figure 5 are results of such simulations. The parameters used for the simulation are listed in Table III. The experimental spectra appear to be broader than the theoretical simulations. This broadening is most likely due to intrinsic heterogeneity of the molecule,[22,50] which results in distributions of the **g** tensor and the **A** tensor. These distributions, in turn, broaden both the EPR and the Mössbauer spectra. This effect of heterogeneity has been discussed in detail by Salerno in the analysis of the EPR spectra of the cytochromes in ubiquinol–cytochrome oxidoreductase (mitochondrial complex III)[22] and has been successfully applied by Dwivedi et al. to simulate the Mössbauer spectra of cytochrome c_{551}.[50] However, such detailed simulations were not performed in our analysis. To accommodate some of the experimental broadening, we have chosen a line width of 0.5 mm/s for the simulations shown in Figure 5.

We note that the theoretical spectra do not fit the experimental data in the central region. It is obvious from the spectra in Figure 5A,B that even at 4.2 K a small amount of the compound remains fast relaxing, resulting in a quadrupole doublet (marked by bracket) similar to that observed at high temperature (Figure 4A). The nature of this fast-relaxing species is unknown. However, its intensity varies with sample preparation and length of room-temperature exposure to the dimethylformamide solvent. Although cleaner EPR spectra were obtained in chlorinated solvents (CH_2Cl_2, $CHCl_3$), these solvents were not suitable for the Mössbauer spectroscopic studies because of absorption of the γ rays by the high concentration of chlorine atoms.

(50) Dwivedi, A.; Toscano, W. A.; Debrunner, P. G. *Biochim. Biophys. Acta* **1979**, *576*, 502–508.

To estimate the values for g_x and g_y, we adopted the crystal field theory that was developed by Griffith[51] to explain the observed g values for low-spin ferric compounds and extended by Oosterhuis and Lang[52] to calculate the Mössbauer hyperfine parameters. This theory assumes that the electronic state of a low-spin ferric compound can be described as a single-electron hole occupying one of the t_{2g} orbitals resulting in three low-lying Kramers' doublets. The energy separations of these three doublets are parameterized in terms of the axial and rhombic field parameters, Δ and V, respectively. These three Kramers' doublets are mixed by the spin–orbit interaction, $-\lambda\vec{L}\cdot\vec{S}$. At low temperature, the EPR and Mössbauer data result from the lowest doublet. An orbital reduction factor, k, was introduced to account for the ligand-binding effects to the 3d orbitals. An overall scaling factor, P, and a Fermi contact factor, κ, were also introduced to calculate the magnetic hyperfine interaction. For heme compounds κ was found to be 0.35 and P approximately 620 kG.[53] Since both g_x and g_y are undetermined, a relation between the three principal g values is required for the data analysis. To achieve this goal, we have chosen two alternative approaches. The first approach is to assume that the orbital reduction factor k equals 1 (i.e., no mixing of the 3d orbitals with the ligand orbitals). this assumption is based on EPR studies of numerous low-spin ferric heme compounds, which indicate that the k value is very close to 1.0. (For example, a value of 1.00 ± 0.05 for k was quoted in ref 22, and values of 1.00 ± 0.01 were found for model heme complexes related to this study.[29]) For $k = 1$, the following relation for the three principal g values can be derived from the Griffith theorem:[54]

$$g_x^2 + g_y^2 + g_z^2 - g_xg_y - g_xg_z + g_yg_z + 4g_x - 4g_y - 4g_z = 0 \quad (2)$$

The second approach is to assume that

$$g_x^2 + g_y^2 + g_z^2 = 16 \quad (3)$$

On the basis of Griffith's theorem, De Vries and Albracht[55] have shown that eq 3 is a limiting case for low-spin ferric compounds and a good approximation for compounds with g_{max} larger than 3.0. Fixing g_z at 3.41 and assuming either eq 2 or 3 is valid, we applied Griffith's theorem and searched for a set of g values that yielded hyperfine parameters in agreement with experiment. It was found that the two approaches give almost identical results (see Table III). The sets of g values found were $g_x = 0.82$, $g_y = 1.87$, and $g_z = 3.41$ for the assumption $k = 1$ and $g_x = 0.85$, $g_y = 1.93$, and $g_z = 3.41$ for the assumption expressed by eq 3. Both approaches yielded crystal field parameters $\Delta = 3\lambda$ and $V = 0.9\lambda$. It is important to realize that once the value of g_z has been measured in the EPR experiment, g_x and g_y can be deduced confidently from the Mössbauer spectra. This is so because the hyperfine parameter A_z, which can be determined with good accuracy from the total splitting of the Mössbauer spectrum, is sensitive to g_y and g_x. For example, with $k = 1$, when g_y varies from 1.82 to 1.88 (the g_x value can be calculated from eq 2), A_z varies from 805 to 825 kG. This is about half the experimental error assigned to A_z (Table III). Hence, we should assign approximate errors of at least ±0.06 to the calculated values of g_x and g_y.

For the above analysis, rhombic symmetry was assumed. With this assumption, data analysis is relatively simple because the **g** tensor and the **A** tensor share a common principal axis system. In reality, one may expect that the symmetry could be lower than rhombic. However, since single-crystal experiments have not been performed on this compound, introducing a lower symmetry would only complicate the situation and would not help in gaining further insight into the electronic properties of this compound.

The Griffith theorem may also be used to calculate the electric field gradient tensor. However, since the theorem takes into consideration only the five 3d electrons, the ligand contributions are neglected. Consequently, it is not surprising that the calculated value of $\Delta E_Q = 2.8$ mm/s is substantially different from the experimental value of 1.7 mm/s. The agreement between the calculated and the experimental values of η should be considered fortuitous.

Discussion

In this work we have shown that although only one feature is clearly resolved in the EPR spectra of the strong g_{max} type of low-spin Fe(III) heme complex, Mössbauer data allow estimation of the other two g values. Previous workers who have observed the anomalously shaped EPR spectra of the strong g_{max} type in model compounds have either misassigned the values of g_y and g_x to impurities present in the samples,[46] reported only the major feature,[30] or attempted to estimate g_y and g_x from spectra recorded in the second-derivative first-harmonic mode[56] or from normal EPR spectra, assuming that g_x is centered at the bottom of the broad valley at ca. 5000–6500 G and that $g_x^2 + g_y^2 + g_z^2 = 16$.[29] The present Mössbauer spectral analysis provides a more reliable means of estimating g_y and g_x, which in turn allows estimation of V and Δ, as discussed below. The danger in equating the value of g_{max} observed in frozen solution with axial ligand plane orientation found in the crystalline state[31] is well illustrated by the case of (OEP)Fe(2-MeImH)$_2^+$ (Figure 3): The crystal structure reported was that of a *high*-spin complex having its axial ligand planes parallel and lying at an angle of 22° to the N_1–N_3 axis,[33] while the same sample, when dissolved in CH_2Cl_2, yields a low-spin strong g_{max} EPR signal, as shown in Figure 3.

The values of the tetragonal and rhombic splitting parameters, Δ and V, respectively, can be calculated from the g values derived from analysis of the Mössbauer spectrum. The value of Δ obtained, 2.188λ (Table III), is somewhat smaller than those obtained from normal B-hemichrome model compounds.[29] For example, the (TPP)Fe^{III} complex with 4-MeImH, the most similar in ligand basicity to 2-MeImH, of imidazole derivatives previously studied,[29] has a value of $\Delta = 3.32\lambda$, while the complexes with ImH and 4-phenylimidazole have slightly smaller values of Δ (3.24λ and 3.12λ, respectively[29]). The smaller value of Δ for the 2-MeImH complex of this study is consistent with a slightly weaker ligand field being provided by 2-MeImH, due to the slightly longer Fe–N_{ax} bonds necessary to accommodate this sterically hindered imidazole ligand (Tables I and II, ref 38). The significantly smaller rhombic splitting for this complex, $V \sim 0.9\lambda$ (Table III), as compared to nonhindered imidazoles, where $V \sim 2\lambda$,[29] is consistent with the near-perpendicular alignment of the axial ligand planes.

It should be pointed out that the values of V and Δ reported in Table III of ref 29 for sterically hindered imidazole and high-basicity pyridine complexes are thus incorrect. These values were obtained by assuming that the minimum g value was about 1.2 (the center of the broad trough at about 5500 G at X-band) and then calculating g_y from eq 3.[29] From the value of g_x obtained from analysis of the Mössbauer spectrum of Figure 5, the g_x feature should be located between 7600 and 7900 G at X-band. Clearly, from inspection of Figure 1 of this work or Figure 3 of ref 29, there is no evidence of the g_x feature in this field region. This is also true of the S-band EPR spectrum (not shown) at the analogous field region, although the width of the g_{max} signal is markedly decreased at S-band. Such loss of spectral resolution is often attributed to "g strain",[22] in which inherent molecular heterogeneity of the sample results in distributions of g values. Salerno has shown[22] that in order to simulate the EPR line shape of the usually lopsided strong g_{max} feature of heme proteins it is necessary to utilize a distribution of rhombicity values, which leads to an unobservably broad spread of g values at g_x and g_y. In Salerno's view the strong g_{max} species *do not have* well-defined

(51) Griffith, J. S. *Mol. Phys.* **1971**, *21*, 135–139.
(52) Oosterhuis, W. T.; Lang, G. *Phys. Rev.* **1969**, *178*, 439–456.
(53) Rhynard, D.; Lang, G.; Spartalian, K. *J. Chem. Phys.* **1979**, *71*, 3715–3721.
(54) Bohan, T. L. *J. Magn. Reson.* **1977**, *26*, 109–118.
(55) De Vries, S.; Albracht, S. P. J. *Biochim. Biophys. Acta* **1979**, *546*, 334–340.
(56) Salerno, J. C.; Leigh, J. S. *J. Am. Chem. Soc.* **1984**, *106*, 2156–2159.

values of g_y and g_x.[57] However, analysis of the Mössbauer spectrum of Figure 5 implies that our complex does have well-defined values of g_x and g_y. From our estimated error limit of ±0.06 it is clear that *some* distribution of g values is likely. It is also possible that we have underestimated the error in the calculated g_x and g_y values by up to perhaps a factor of 2, which would be consistent with the occurrence of a greater distribution of g values. It would be interesting to simulate the EPR spectrum as a function of the g values obtained from analysis of the Mössbauer spectrum and as a function of distributions about those g_x and g_y values. Such a distribution of g values could easily be expected in the present case if there is a distribution of angular alignment of axial ligand planes. However, even in the crystalline form of (TPP)Fe(2-MeImH)$_2^+$, where the distribution of angles is probably much smaller than in frozen glassy solution, there is no evidence of g_y or g_x (Figure 1).

It is also worth pointing out that even if the axial ligands of (TPP)Fe(2-MeImH)$_2^+$ are assumed to be identically aligned in every molecular unit, they are known not to be aligned in planes oriented perfectly at 90°, but rather at 89°.[38] Likewise, the g values calculated from the Mössbauer spectra of Figure 5 are not axial (Table III), but rather lead to the above-mentioned calculated rhombic splitting parameter $V \sim 0.9\lambda$ (Table III). From these results it is tempting to suppose that the relationship between axial ligand plane orientation and g_y and g_x values is a steep function of angle as the ideal perpendicular orientation is approached, for example, that $(g_y - g_x)\alpha \log \cos^2 \theta$. Such a steep function would also help to explain the observed g strain.

The new crystalline sample of (TPP)Fe(ImH)$_2^+$Cl$^-$, for which pertinent structural data are summarized in Table II, exhibited two closely spaced "normal" B-hemichrome EPR signals, with g_{max} = 3.00 and 2.84 (cf. Figure 2). The X-ray structure determination provides an explanation for the two different EPR signals. Crystals of this "new" phase contain two distinct molecular sites, each having a required inversion center for the (TPP)Fe(ImH)$_2^+$ ion. The two sites differ primarily in the orientation of the imidazole planes with respect to the N_1–N_3 vector; the inversion center requires that the imidazole planes in each molecule are parallel. One molecule has the two parallel axial ligands at an angle of 6° from the N_1–N_3 porphinato vector, and the other has parallel axial ligands at an angle of 41° to the N_1–N_3 vector[49,58] (Table II). Hence, it appears that, all other things being equal, subtle differences in g value may be attributable to the relative orientation of the porphinato nitrogen and axial ligand plane vectors. However, the results make clear that *even a very unusual parallel orientation (41°) does not give rise to a strong g_{max} EPR spectrum.* (Interestingly, this new crystalline phase of (TPP)Fe(ImH)$_2^+$Cl$^-$ was obtained in our efforts to repeat the preparation of the phase reported by Hoard many years ago.[37] This structure was one of the two exceptions to the rule that axial ligands prefer to be aligned in parallel planes (Table I) when this study was undertaken, and on the basis of our results involving the 2-methylimidazole complex, we suspected that these crystals should have g_{max} greater than 3.0. Unfortunately, it has not thus far been possible to grow crystals of the form on which the first crystal structure was done.) It should also be noted that the glassy-solution EPR results for the bis(2-methylimidazole) complex are essentially the same as those for the crystalline sample, indicating that the crystalline sample has the thermodynamically preferred axial ligand plane orientations. However, for the bis(imidazole) complex, frozen-solution EPR results[29] indicate only one species present, while EPR spectra of the crystals indicate two, one of which has very similar parameters to those in the frozen solutions (g_z = 2.87, g_y = 2.29, g_x 1.56[29]), suggesting that one of the parallel axial ligand orientations observed in the crystal is preferred thermodynamically.[62]

To summarize the above discussion, we have been able to characterize structurally three of the four possible extremes of axial ligand orientation in low-spin iron(III) porphyrins: (1) ligands in parallel planes, lying over the nitrogens ($\Theta = 0°$, $\varphi \sim 0°$); (2) ligands in parallel planes, lying over the meso positions ($\Theta = 0°$, $\varphi \sim 45°$); (3) ligands in perpendicular planes, lying over the meso positions ($\Theta \sim 90°$, $\varphi \sim 45°$). The first two, with ligands in parallel planes, result in normal B-hemichrome EPR signals, with all three g values resolved (Figure 2). The third, with ligands in perpendicular planes over the meso positions, results in a strong g_{max} EPR signal, with unresolved g_x and g_y components (Figure 1). It would be difficult to design a model heme complex of the fourth possible case, i.e., having axial ligands in perpendicular planes lying over the nitrogens ($\Theta = 90°$, $\varphi = 0°$), since it appears that parallel orientation of axial ligand planes is the thermodynamically favored, in the absence of steric hindrance from the axial ligands. [Placing 2-MeImH nearly over the porphyrin nitrogens produces a high-spin complex[33] when the ligands are in parallel planes, and likely also if the ligands were in perpendicular planes, since to shorten the Fe–N_{ax} bond length to the point where spin crossover could occur would require displacing alternate porphyrin nitrogens above and below the mean plane of the porphyrin ring, an unlikely alternative to simply rotating each ligand by 45°, as observed for the 2-MeImH complex of (TPP)Fe^{III}.[38]] However, in biological samples it is possible that axial ligands could be held in this fourth orientation by hydrogen-bonding networks within the protein. Although we have no model compound of this type, we predict that it would also exhibit a strong g_{max} signal, on the basis of the similarity between the two cases (1 and 2) of parallel-aligned axial ligands. Hence, we believe that it is reasonable to assume that if a strong g_{max} EPR signal is observed, the imidazole ligands are oriented in perpendicular planes. The strong g_{max} EPR signal is thus indicative of near-axial symmetry of the heme group under investigation.

For biological samples, the strong g_{max} signal is the only observable feature of a number of low-spin Fe(III) hemes, including the mitochondrial cytochromes b and c_1 of complex III. The g values of both intact complex III and cytochrome b isolated from complex III of mitochondria of higher animals and of yeast and the similar complexes found in photosystems I and II of chloroplasts have been reported by a number of workers over the years. These are difficult systems with which to work, which accounts for some of the variation in EPR and redox potential results that have been reported. Selected EPR and electrochemical data,

(57) Salerno, J. C., personal communication.

(58) It is interesting to note that the molecule with larger φ angle has essentially identical Fe–N_P bond distances (1.990–1.995 Å), while the molecule with a small φ angle has a rhombic distortion of the porphinato core, with long Fe–N_P distances (2.002 Å) parallel to the imidazole ligands and short Fe–N_P distances (1.985 Å) perpendicular to the imidazole planes. Such a static distortion is consistent with the dominant π interaction of low-spin Fe(III) with both porphyrin and axial ligand being of the L → M π back-bonding type, as found in NMR studies of low-spin Fe(III) porphyrins.[59,60] Hence, we expect the unpaired electron of the (TPP)FeIm$_2^+$ unit with small φ to be in the d_π orbital which is perpendicular to the imidazole planes, so that both imidazole and porphyrin can (in principle, at least) donate π-electron density to the remaining hole in this d_π orbital. The fact that the Fe–N_P bonds along this axis are shorter than those parallel to the imidazole ligands suggests that the amount of Por → Fe π back-bonding is significant. In comparison, the high-spin crystalline form of (OEP)Fe(2-MeIm)$_2^+$, in which the axial ligands are also in parallel planes with small φ angle[33] (Table I), has the opposite rhombic distortion, with the short Fe–N_P bonds *parallel* to the axial ligands. This is consistent with the fact that NMR studies[59,61] have shown that the mechanism of spin delocalization in high-spin Fe(III) porphyrins as $M(d_\pi) \rightarrow L(\pi^*)$. Since the metal orbitals are only half-filled, the porphyrin and imidazole ligands would compete for the metal π electron along the Fe–N_P axis perpendicular to the 2-methylimidazole ligands. No such competition could occur along the Fe–N_P axis parallel to the 2-methylimidazole planes for symmetry reasons, so Fe → Por bonding should be stronger and the bonds shorter, as observed.

(59) Walker, F. A.; LaMar, G. N. *Ann. N.Y. Acad. Sci.* **1973**, *206*, 328–348.

(60) LaMar, G. N.; Walker, F. A. *J. Am. Chem. Soc.* **1973**, *95*, 1782–1790.

(61) LaMar, G. N.; Eaton, G. R.; Holm, R. H.; Walker, F. A. *J. Am. Chem. Soc.* **1973**, *95*, 63–75.

(62) It is tempting to speculate that the crystalline species having g_z = 2.84, g_y = 2.32, and g_x = 1.59 and hence Δ = 3.12 λ and V = 2.16 λ (weaker tetragonal field, larger rhombic splitting) is due to the molecules having a small φ angle (6°) and longer Fe–N_{ax} bonds, while the species having g_z = 3.00, g_y = 2.2, and g_x = 1.47 and hence Δ = 3.53 λ and V = 1.72 λ (stronger tetragonal field, smaller rhombic splitting) is due to the molecules with a large φ angle (41°) and shorter Fe–N_{ax} bonds. If true, this leads to the conclusion that a small φ angle is thermodynamically favored.

Table IV. Redox Potentials and EPR Parameters of the Cytochromes of Mitochondrial Complex III and the Isolated Components

source/prepn	pH	*T*, K	$\epsilon°$,[a] mV vs. NHE	g_{max}	ref
bovine heart/mitochondria	7.0	298			21
b_{562}			105		
b_{565}			5		
bovine heart/membrane bound	7.2				19
b_{562}			93		
b_{565}			−34		
bovine heart/isolated cyt *b*	7.0	rt	−5, −85		21
pigeon breast/sol in phospholipid	7.2	298			20
b_{561}			95	3.41	
b_{566}			0	3.78	
pigeon breast/sol in cholate/Triton X-100	7.2				18
b_{561}			55	3.44	
b_{566}			−40	3.78	
complex III/unspecified					22
b_{562}				3.44	
b_{566}				3.75	
yeast complex III/intact	7.4	297			23
b_{562}			62		
b_{566}			−20		
yeast cyt *b*/isolated	7.4	297	−44 (2)		24
chloroplasts	7.3	rt			
photosystem I/isolated b_{563} (b_6)			+70, −50	3.5, 3.6–3.7	25
photosystem I/denaturated b_{563} (b_6)				2.9	25
photosystem II					
b_{559}, high-pot. form	7.0	rt	400	3.08	17
b_{559}, low-pot. form			0	2.94	17

[a] Potentials relative to NHE. Ionic strength not specified.

representative of the most commonly observed results for *b*-type cytochromes, are listed in Table IV. The three hemes of complex III are all low-spin ferrihemes having only one observable feature to their EPR spectra: a strong g_{max} signal at $g = 3.33$ for c_1, 3.44 for b_{562} (b_K), and 3.78 for b_{566} (b_T). While the investigators who first reported these EPR spectra[27] did not speculate on the identity of the axial ligands bound to Fe(III), it was often assumed by others, on the basis of EPR spectra obtained by addition of aliphatic amines to the monomeric glycera hemoglobin[63] and to leghemoglobin,[64] as well as those obtained upon pH titrations of cytochrome *c*,[65] that all of these membrane-bound cytochromes of complex III must have at least one aliphatic amine bound to Fe(III) and that b_T must have two aliphatic amines as the axial ligands. However, it seems unnecessary to assume axial coordination of aliphatic amines in the membrane-bound cytochromes of complex III, based on reports by Palmer and co-workers[30] and Migita and Iwaizumi[46] that a $g = 3.4$ signal of the strong g_{max} type could be generated from ferriprotoporphyrin in the presence of 2-methylimidazole. Perusal of the literature[63-75] indicates a significant number of heme proteins have strong g_{max} signals, either in their native states or in the presence of specific modifying agents such as CN^-, pyridines, or aliphatic amines.

Recent work of Widger and co-workers[16] has shed important light on the question of the identity of the axial ligands of cytochrome *b* by showing that the amino acid sequence of cytochromes *b* from five different mitochondrial sources and a chloroplast cytochrome b_6 all have four histidines in similar positions in the sequence. These workers further showed, by calculations of the most likely folding patternhs of these proteins, that the two hemes appear to reside on opposite sides of the hydrophobic intramembrane protein core, each bound to two histidines. The two histidines bound to each heme are located on quite different parts of the polypeptide, which apparently folds in such a way as to bring the α-helices containing each of these histidines into proximity for binding to the appropriate heme.[16] Hence, the axial ligands of cytochromes b_T and b_K appear to be two histidine imidazoles, as is also true of the cytochromes b_5 obtained from erythrocytes[9] ($E_{m,7} = -2$ mV[10]), liver microsomes[7] ($E_{m,7} = 10$–20 mV,[8] depending on source and treatment), and cytochrome b_2 of bakers' yeast[11] ($E_{m,7} = -12$ mV[12]). In spite of this common axial coordination and similar redox potentials, the EPR spectra of the "cytochrome b_2 core"[13] and the cytochromes b_5[14] are those of typical B-hemichromes,[15] while those of the mitochondrial cytochromes b_T and b_K are characterized by the strong g_{max} feature at $g > 3$.[25]

More recently, Babcock and co-workers[17] have shown that chloroplast b_{559}, a membrane protein intrinsic to the core complex of photosystem II, probably consists of two polypeptides, each of which provides a histidine for coordination to the heme, which thus acts as a bridge between the two polypeptides. Under certain conditions the membrane-bound b_{559} can exist in two states: a high-potential form ($E_{m,7} \sim 400$ mV) or a variety of low-potential forms having $E_{m,7} \sim 0$ mV as a lower bound.[17] High-potential b_{559} has $g_z = 3.08$ and $g_y = 2.16$, whereas the low-potential forms have $g_z = 2.94$ and $g_y = 2.26$.[17] The isolated and purified form has low potential, and $g_z = 2.94$.[17] These workers suggest that the source of the difference in the redox potentials and *g* values is a difference in the angular orientation of the axial imidazole ligands but that the physiologically relevant form of the protein is that which has an unusual, strained configuration of the two axial histidines, probably a perpendicular orientation of the imidazole planes.[17] However, it should be noted that the value of g_z of the high-potential form of b_{559} is not as large as those of the strong g_{max} species (cytochromes *b* from mitochondrial complex

(63) Seamonds, B.; Blumberg, W. E.; Peisach, J. *Biochim. Biophys. Acta* **1972**, *263*, 507–514.
(64) Appleby, C. A.; Blumberg, W. E.; Peisach, J.; Wittenberg, B. A.; Wittenberg, J. B. *J. Biol. Chem.* **1976**, *251*, 6090–6096.
(65) Brautigan, B. L.; Feinberg, B. A.; Hoffman, B. M.; Margoliash, E.; Peisach, J.; Blumberg, W. E. *J. Biol. Chem.* **1977**, *252*, 574–582.
(66) Siedow, J. N.; Vickery, L. E.; Palmer, G. *Arch. Biochem. Biophys.* **1980**, *203*, 101–107.
(67) Chao, Y.-Y. H.; Bersohn, R.; Aisen, P. *Biochemistry* **1979**, *18*, 774–779.
(68) Muhoberac, B. B.; Wharton, D. C. *J. Biol. Chem.* **1983**, *258*, 3019–3027.
(69) Ellfolk, N.; Ronnberg, M.; Aasa, R.; Andreasson, L.-E.; Vanngard, T. *Biochim. Biophys. Acta* **1983**, *743*, 23–30.
(70) T'sai, A.-H.; Palmer, G. *Biochim. Biophys. Acta* **1982**, *681*, 484–495.
(71) Cammack, R.; Fauque, G.; Moura, J. J. G.; LeGall, J. *Biochim. Biophys. Acta* **1984**, *784*, 68–74.
(72) DerVartanian, D. V.; LeGall, J. *Biochim. Biophys. Acta* **1971**, *243*, 53–65.
(73) Foote, N.; Peterson, J.; Gadsby, P. M. A.; Greenwood, C.; Thomson, A. J. *Biochem. J.* **1984**, *223*, 369–378.
(74) Orme-Johnson, N. R.; Hansen, R. E.; Beinert, H. *Biochem. Biophys. Res. Commun.* **1971**, *45*, 871–878.
(75) Brudvig, G. W.; Stevens, T. H.; Morse, R. M.; Chan, S. I. *Biochemistry* **1981**, *20*, 3912–3921.

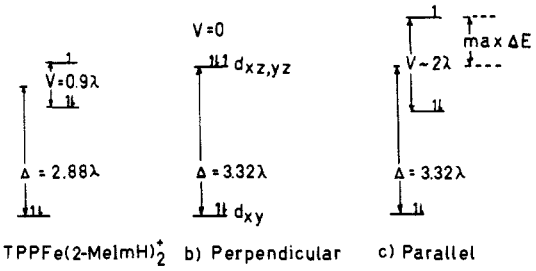

Figure 6. Schematic representation of the energy level diagram of the three t_{2g} orbitals of LS Fe(III): (A) the case of (TPP)Fe(2-MeImH)$_2^+$, $\Delta \sim 2.88\lambda$, $V \sim 0.9\lambda$, as determined from the Mössbauer and EPR experiments reported herein; (B) the ideal case of perpendicularly oriented axial ligand planes, $V = 0$; (C) the case of (TPP)Fe(4-MeImH)$_2^+$, $V \sim 2\lambda$. The tetragonal splitting is assumed constant at $\Delta = 3.32\lambda$[22] for cases B and C. Note that if $\Delta E = \Delta G = -nF\epsilon^0$, then the maximum $\Delta\epsilon^0$ = 50 mV if $\lambda = 400$ cm^{-1}.[76]

III or chloroplast b_6f complex) nor is the shape the same. Specifically, g_y is resolved.

Salerno[22] has recently demonstrated that strong g_{max} EPR signals for bis(histidine)-coordinated hemins can be simulated by assuming that the tetragonal field, Δ, of the axial imidazoles remains at ca. 3.32λ, irrespective of the value of g_{max}, and that the anomalous line shape is due to "g strain", which gives rise to a range of molecular conformations that in turn give rise to a distribution of g values. Salerno calculates the three g values as a function of the rhombic splitting parameter, V, keeping Δ fixed at 3.32λ; for $V = 0$, g_z approaches a maximum value of slightly greater than 3.8.[54,57] Changes in V give rise to much larger changes in g value than changes in Δ except very near $V = 0$. When V was varied about an average value while Δ was held constant, the line shapes of the cytochrome b_T, b_K, and c_1 EPR signals (with $\Delta = 2.5\lambda$ for c_1, assuming it has His–Met ligation) were simulated in good agreement with the observed shapes of the signals.[22] Although in principle one could obtain the other two g values from this analysis, it is unlikely that the simulation technique would lead to determination of these values to high accuracy.

On the basis of Salerno's idea of a fairly constant value of the tetragonal field parameter, Δ, independent of axial ligand plane orientation, the question arises as to whether realistic variations in the rhombic splitting parameter, V, could lead to variations in redox potential similar to those observed (Table IV). Assuming the tetragonal splitting to be 3.32λ, as observed for (TPP)Fe(4-MeImH)$_2^+$,[29] and that the rhombic splitting can be no larger than that observed for normal B-hemichromes, i.e., ca. 2λ, where the axial ligand planes are parallel, and that it can drop to zero when the axial ligand planes are forced to be perpendicular, the maximum variation in the energy of the highest d orbital, into which the electron goes upon reduction, is $2\lambda/2$, or λ. Assuming that λ for low-spin Fe(III) is probably not larger than 400 cm^{-1} when surrounded by four porphyrin nitrogens and two axial imidazoles,[76] the maximum difference in energy of the highest energy d orbital of the parallel and perpendicular forms cannot thus be more than ca. 400 cm^{-1} (cf. Figure 6). The parallel (large V) orientation has this orbital at higher energy (Figure 6). This translates into a possible redox potential difference of ca. 50 mV, with the perpendicular ($V = 0$) orientation producing the more positive ϵ^0, since $\Delta G = -nF\epsilon^0$. While this difference is small compared to the measured difference in redox potential of b_{562} and b_{566} hemes in intact mitochondria (Table IV), it is in the right direction and similar in magnitude to the difference in redox potential for each b heme between intact mitochondria and isolated cytochromes b (Table IV) and could be an important factor in fine tuning the redox potentials of complex III in the presence of possible membrane-modifying or -denaturing substances.

It thus appears reasonable, as suggested by Babcock and coworkers,[17] that chloroplast cytochrome b_{559} has undergone some reorganization upon isolation in the low-potential form, part, *but not all*, of which *may* be due to allowing the axial ligands to "relax" into their "nonstrained" (i.e., parallel) orientation. (The observed drop of 400 mV on going from native to isolated forms of b_{559} is clearly far too large to be attributed solely to the change in axial ligand plane orientation, as shown in Figure 6.) As for the difference in redox potential between b_{562} and b_{566}, both of which have strong g_{max} EPR signals and thus probably also perpendicularly oriented axial ligand planes, another important factor must contribute significantly to determining the value of the redox potentials. One likely candidate for these membrane-bound hemes is hydrogen bonding of the buried histidine N^1 H protons to protein residues or the presence of buried polar or charged groups. The effect of H bonding and imidazole deprotonation have been probed in model compounds by both Sweigert[77] and Valentine[78] and have been shown to lead to large negative shifts in Fe(III)/Fe(II) redox potential as the degree of deprotonation increases. The effect of buried polar or charged groups on redox potentials and the stabilization of charges at or very near the iron center is potentially large, as indicated by the calculations of Moore for cytochromes c and c_2.[79]

In line with this latter suggestion, it should be pointed out that the tetraheme protein cytochrome c_3 from *Desulfovibrio desulfuricans* strain Norway has two low-spin Fe(III) EPR signals in an intensity ratio of approximately 3:1. The signal from the major species is that of a "normal" B-hemichrome, with $g_{max} \sim 3.0$, while the minor species has $g_{max} = 3.36$.[71] This latter signal has been ascribed to the lowest potential heme.[71] The X-ray crystal structure shows that three hemes have their axial histidine imidazoles in approximately parallel planes, while one ("heme 1") has its axial imidazoles in perpendicular planes.[2] However, this heme is one of the least exposed to the aqueous medium,[2] and in this very small protein containing four hemes, exposure (or lack thereof) to the aqueous environment[80] might be expected to be the most important factor, hence leading the fourth heme to have higher rather than lower redox potential, in contradiction to the observed correlation between redox potential and g value.[71] Furthermore, the arguments based on axial ligand orientation, presented in the previous paragraphs and Figure 5, also suggest that the heme having the largest value of g_{max} should have the most positive, rather than the most negative, redox potential as observed.[71] However, an important factor in this case could be the strengths of the hydrogen bonds to the NH protons of the histidine imidazoles coordinated to heme 1, which are provided by protein side chains (Ser-86 and Gln-29) rather than protein backbone amide oxygens, as in the majority of the other hemes.[2] Thus, the axial ligands of heme 1 could be more imidazolate-like, leading to lower relative redox potential.[77,78] However, this interpretation is in disagreement with the EPR data, since imidazolate-coordinated hemes give "H-hemichrome" EPR spectra, with $g_{max} = 2.8$,[15,29] although the effect of imidazole deprotonation on the EPR parameters of sterically hindered imidazoles has yet to be reported. Such investigations are currently under way. Clearly, the assignment and interpretation of redox potentials and g values of cytochrome c_3 hemes with structural features of the molecule bear further study.

Hence, it appears that the orientation of axial ligand planes is one of the factors that can affect the redox potentials of heme

(76) The free-ion single-electron spin–orbit coupling constant for Fe(III) has been given as 460 cm^{-1} (Figgis, B. N.; Lewis, J. In *Techniques of Inorganic Chemistry*; Jonassen, H. B., Weissberger, A., Eds.; Wiley Interscience: New York, 1965; Vol. IV, p 159). For low-spin Fe(III) this would mean λ = 460 cm^{-1}. However, for complexes with strong-field ligands such as porphyrins and imidazoles, it is reasonable to expect that λ will be reduced by covalency. Maltempo (Maltempo, M. M. *J. Phys. Chem.* **1974**, *61*, 2540–2547) has used the value 300 cm^{-1} for low-spin ferrihemes. We have used 400 cm^{-1} in this work as the maximum possible value of λ for order-of-magnitude estimates of the effect of rhombic symmetry on redox potential.

(77) Doeff, M. M.; Sweigert, D. A.; O'Brien, P. *Inorg. Chem.* **1983**, *22*, 851–852. O'Brien, P.; Sweigart, D. A. *Inorg. Chem.* **1985**, *24*, 1405–1409.

(78) Quinn, R.; Mercer-Smith, J.; Burstyn, J. N.; Valentine, J. S. *J. Am. Chem. Soc.* **1984**, *106*, 4136–4144.

(79) Moore, G. R.; Harris, D. E.; Leitch, F. A.; Pettigrew, G. W. *Biochim. Biophys. Acta* **1984**, *764*, 331–342.

(80) Stellwagen, E. *Nature (London)* **1978**, *275*, 73–74.

proteins. Other factors that have been enumerated in this paper and have been addressed directly by us or others include heme substituents,[1,81] identity of the axial ligands,[1,82] hydrogen bonding of the imidazole NH to protein residues,[77,78] the presence of polar or charged groups near the heme,[79] and exposure to the aqueous environment.[80] Apportioning the appropriate contribution of each of these factors to the observed redox potential of each heme protein is a difficult undertaking.

It should also be pointed out that since Fe(III) porphyrins with perpendicularly aligned axial ligand planes produce strong g_{max} EPR signals, one can also predict that (Por)Fe$(CN)_2^-$ should likewise have such an EPR signal, with g_z large and $g_x = g_y$ and very small, since the cylindrical axial ligand symmetry requires that $V = 0$. Such a signal has recently been observed at very low temperatures for a crystalline sample,[83] and we have observed a sharp strong g_{max} signal at $g = 3.81$ for (TPP)Fe$(CN)_2^-$ in DMF glasses at 7 K. A similar EPR signal was observed when *N*-MeIm + CN^- were added to (TPP)FeI in DMF and cooled to 7 K.[84] The fact that the mono(cyano) complexes of several heme proteins, including the a_3 heme of cytochrome oxidase, have also been reported to have strong g_{max} EPR signals, observable only at very low temperatures,[73,75] suggests that cyanide so strongly dominates the electronic properties of the metal that it imposes effective axial symmetry in spite of the presence of the histidine imidazole plane of the other axial ligand.

Lastly, with regard to model compounds, one might ask how the interpretation presented here of the strong g_{max} EPR signal in terms of perpendicular alignment of axial ligand planes can be used to explain the observed[29] change in behavior of bis(pyridine)-coordinated Fe(III) porphyrins as a function of the basicity of the pyridine ligands. It was found that Fe(III)–porphyrin complexes with high-basicity pyridines [p$K_a(BH^+) > 8.1$] exhibit the same "normal" B-hemichrome EPR spectra as do the complexes with nonhindered imidazoles, while the complexes with "low-basicity pyridines" [p$K_a(BH^+) < 7.4$] have strong g_{max} EPR signals, as do the Fe(III)–porphyrin complexes with hindered imidazoles.[29] According to the present interpretation, then, the "high-basicity" pyridines must form complexes having their axial ligands in parallel planes in the frozen glasses used for these previous investigations, while "low-basicity" pyridines must form complexes having their axial ligands in perpendicular planes. The only crystal structure that has been reported for a bis(pyridine)iron–porphyrinate complex is that of the (OEP)Fe(3-Clpy)$_2^+$, which although it has its axial ligands in parallel planes, has very long Fe–N_{ax} bonds and is intermediate spin[34b] (Table I). Thus, this particular form does not answer the question as to axial ligand plane alignment in *low-spin* bis(pyridine) complexes of iron porphyrinates. Further studies are in progress. Interestingly, as pointed out previously,[29] only the high-basicity pyridines have their filled π orbitals at higher energy than the lone-pair orbital,[85] thus making them strong π-donor ligands, as are the imidazoles.[29,86] This may suggest an important role for π donation from the axial ligands in maintaining parallel axial ligand planes and, hence, low redox potentials. Further studies are in progress to test this hypothesis. Interestingly, NMR studies of cytochromes *c* from various species have implicated the axial methionine sulfur π-symmetry lone pair as an important factor in determining heme electronic anisotropy.[87] One might also wonder whether this lone pair plays a role in determining the redox potentials of those cytochromes *c*, which have his/met ligation.

Conclusions

We have demonstrated, by combined EPR, Mössbauer, and X-ray crystallographic investigations, that strong g_{max} EPR signals of low-spin Fe(III) porphyrins can be correlated with perpendicularly aligned axial imidazole planes and that Mössbauer spectroscopic measurements, together with theoretical calculations and spectral simulations, can lead to estimation of the other two (unobserved) *g* values. We have also shown, from crystal field analysis, that perpendicular alignment could lead to a positive shift in redox potential of up to about 50 mV over that observed for parallel alignment, all other structural and environmental factors being equal. Hence, axial ligand plane alignment alone cannot account for the extreme positive shifts observed in such proteins as native cytochrome b_{559}.[17]

Acknowledgment. We thank Dr. D. V. DerVartanian for his assistance and hospitality in the use of his laboratory for recording some of the EPR data. We also thank Professor John C. Salerno for many helpful comments and Dr. David Geiger for the original preparation of (TPP)Fe(2-MeIm)$_2$ClO$_4$·THF. We thank the National Institutes of Health for a research career development award (Grant AM 01135) to B.H.H. This work was supported by the National Science Foundation [Grant PCM-8305995 (B.H.H.)] and the National Institutes of Health [Grants AM 31038 (F.A.W.), GM 32187 (B.H.H.), and HL 15627 (W.R.S.)].

Registry No. (TPP)Fe(ImH)$_2^+$Cl$^-$, 68011-15-4; (OEP)Fe(2-MeIm)$_2^+$ClO$_4^-$, 92055-42-0; (TPP)Fe(2-MeImH)$_2^+$, 59910-76-8; (TPP)Fe(4-MeImH)$_2^+$, 59910-77-9; Fe, 7439-89-6; N, 7727-37-9; cytochrome *b*, 9035-37-4.

(81) Walker, F. A.; Barry, J. A.; Balke, V. L.; McDermott, G. A.; Wu, M. Z.; Linde, P. F. *Adv. Chem. Ser.* **1982**, *No. 201*, 377–416.
(82) Kadish, K. M.; Thompson, L. K.; Beroiz, D.; Bottomley, L. A. In *Electrochemical Studies of Biological Systems*; Sawyer, D. T., Ed.; ACS Symposium Series 38; American Chemical Society: Washington, DC, 1977; p 51. Kadish, K. M.; Bottomley, L. A.; Beroiz, D. *Inorg. Chem.* **1978**, *17*, 1124–1129. Kadish, K. M.; Kelly, S. *Inorg. Chem.* **1979**, *18*, 2968–2971.
(83) Strouse, C. E., personal communication.
(84) Walker, F. A., unpublished results.
(85) Ramsey, B. G.; Walker, F. A. *J. Am. Chem. Soc.* **1974**, *96*, 3314–3316.
(86) Ramsey, B. G. *J. Org. Chem.* **1979**, *44*, 2093–2097.
(87) Keller, R. M.; Wuthrich, K. *Biochem. Biophys. Res. Commun.* **1978**, *83*, 1132–1139.